Available online at www.sciencedirect.com
ScienceDirect
Phytochemistry 68 (2007) 2258–2272
PHYTOCHEMISTRY
www.elsevier.com/locate/phytochem

GC-EI-TOF-MS analysis of *in vivo* carbon-partitioning into soluble metabolite pools of higher plants by monitoring isotope dilution after $^{13}CO_2$ labelling

Jan Huege, Ronan Sulpice, Yves Gibon, Jan Lisec, Karin Koehl, Joachim Kopka *

Max Planck Institute of Molecular Plant Physiology, Am Muehlenberg 1, 14476 Potsdam-Golm, Germany

Received 12 January 2007; received in revised form 12 March 2007
Available online 1 May 2007

Abstract

The established GC-EI-TOF-MS method for the profiling of soluble polar metabolites from plant tissue was employed for the kinetic metabolic phenotyping of higher plants. Approximately 100 typical GC-EI-MS mass fragments of trimethylsilylated and methoxyaminated metabolite derivatives were structurally interpreted for mass isotopomer analysis, thus enabling the kinetic study of identified metabolites as well as the so-called functional group monitoring of yet non-identified metabolites. The monitoring of isotope dilution after $^{13}CO_2$ labelling was optimized using *Arabidopsis thaliana* Col-0 or *Oryza sativa* IR57111 plants, which were maximally labelled with ^{13}C. Carbon isotope dilution was evaluated for short (2 h) and long-term (3 days) kinetic measurements of metabolite pools in root and shoots. Both approaches were shown to enable the characterization of metabolite specific partitioning processes and kinetics. Simplifying data reduction schemes comprising calculation of ^{13}C-enrichment from mass isotopomer distributions and of initial ^{13}C-dilution rates were employed. Metabolites exhibited a highly diverse range of metabolite and organ specific half-life of ^{13}C-label in their respective pools (^{13}C-half-life). This observation implied the setting of metabolite specific periods for optimal kinetic monitoring. A current experimental design for the kinetic metabolic phenotyping of higher plants is proposed.

Keywords: *Arabidopsis thaliana* Col-0; *Oryza sativa* IR57111; ^{13}C-carbon; $^{13}CO_2$-carbondioxide; Dynamic flux analysis; Electron impact ionization (EI); Gas chromatography (GC); Metabolite profiling; Stable isotope dilution; Time-of-flight mass spectrometry (TOF-MS)

1. Introduction

The labelling of plants with CO_2 using both radioactive (e.g. Calvin, 1956, 1964) or stable isotope tracing (e.g. Schaefer et al., 1975, 1980; MacLeod et al., 2001; Schwender et al., 2004) has been used since decades utilizing the main entry points of CO_2 into plant metabolism, namely ribulose-1,5-diphosphate carboxylase (EC 4.1.1.39) and phosphoenolpyruvate carboxylase (EC 4.1.1.31). Over time, CO_2 tracing yielded ground-breaking biological insights into photosynthetic carbon assimilation, photorespiration and metabolism and, thus, into essential life-sustaining physiological mechanisms on earth.

With the increasing availability of stable isotopes, methods for the *in vivo* labelling of plants are conceivable. Successful methods for the complete and saturating ^{13}C-labelling were reported previously using a microbial model, such as *Saccharomyces cerevisiae* (Birkemeyer et al., 2005). In this work we present and characterize a method for the full *in vivo* ^{13}C-labelling of higher plants.

Abbreviations: EI, electron impact ionization; GC, gas chromatography; MS, mass spectrometry; MST, mass spectral tag; RI, retention time index; TOF, time-of-flight.

* Corresponding author. Tel.: +49 331 567 8262; fax: +49 331 567 898262.
E-mail address: Kopka@mpimp-golm.mpg.de (J. Kopka).

0031-9422/$ - see front matter © 2007 Elsevier Ltd. All rights reserved.
doi:10.1016/j.phytochem.2007.03.026

With this prerequisite in place isotope dilution after $^{13}CO_2$ labelling was monitored. The kinetic measurement of isotope decay from ^{13}C to ^{12}C can be performed under ambient atmospheric conditions, thus allowing sampling with minimal experimental disturbance. As a consequence experiments with extended kinetic monitoring of CO_2-dilution under diverse regimes of environmental conditions are now conceivable. Thus we aim to contribute to the ongoing discussion and development of empirical flux estimations in the field of plant physiology (e.g. Fernie et al., 2005; Baxter et al., 2007). We specifically intend to work towards dynamic flux estimations (Ratcliffe and Shachar-Hill, 2006) as a tool for the phenotypic analysis of gene function in higher plants.

Besides nuclear magnetic resonance (NMR), mass spectrometric (MS) analysis has traditionally been used for flux analyses, for example MALDI-TOF (e.g. Wittmann and Heinzle, 2001), quadrupole based GC–MS (e.g. Dauner and Sauer, 2000), ion trap mass spectrometry (e.g. Klapa et al., 2003) or LC triple quadrupole mass spectrometry (e.g. van Winden et al., 2005). We employed the widely applied gas chromatography electron impact ionization time-of-flight mass spectrometry, in short GC-EI-TOF-MS technology, for metabolite profiling (e.g. Wagner et al., 2003; Lisec et al., 2006; Erban et al., 2006). GC-EI-TOF-MS is a non-scanning mass spectrometric technology, which allows simultaneous monitoring of a mass range and high acquisition rates of 10–500 mass spectra s^{-1}. Thus apparent fragment ratios are not subject to artefacts caused by the temporal offset of the sequential mass recording, which is inherent to mass scanning technologies, such as the quadrupole or ion trap GC–MS. The feasibility of mass isotopomer monitoring of methoxyaminated and silylated derivatives by GC–MS metabolite profiling has been demonstrated earlier (Roessner-Tunali et al., 2004; Baxter et al., 2007). The decision to use this specific mode of derivatization and analytical monitoring was made in view of the high synergy to be expected of method development and metabolite identification efforts in the metabolite profiling field (e.g. Schauer et al., 2005a). Substantial instrumental progress has also been made, for example by GC×GC-TOF-MS (e.g. Sinha et al., 2004a,b; Kell et al., 2005) implementation. Furthermore, a highly versatile tool box of metabolite fractionation and chemical derivatization schemes awaits exploration (Kopka, 2006a).

In the following study we perform a technological assessment of the combination of mass isotopomer analysis using the GC-EI-TOF-MS profiling method and monitoring of isotope dilution after $^{13}CO_2$ labelling. We specifically address the use of populations of replicate, genetically identical plants for flux studies and describe fundamental technological requirements. First results are presented, which demonstrate the feasibility and potential but also the current limitations of this novel combination of techniques.

2. Results and discussion

2.1. GC-EI-MS fragmentation analysis

The electron impact (EI) fragmentation pattern of trimethylsilylated and methoxiaminated metabolite derivatives (analytes), which are observed in routine metabolite profiles (e.g. Erban et al., 2006; Fiehn et al., 2000a; Lisec et al., 2006; Roessner et al., 2000) delimit the potential of this profiling method for the multi-parallel analysis of metabolic fluxes using ^{13}C-stable isotope dilution. Specifically the targeted retrieval of quantitative mass isotopomer information and the calculation of isotope enrichment from mass isotopomer distributions require the thorough interpretation of GC-EI fragmentation patterns and the knowledge of the sum formula of each analyzed mass fragment. As suggested previously (Birkemeyer et al., 2005), we used mass spectral tags (MSTs; cf. the definition made by Desbrosses et al., 2005 refined by Kopka, 2006b) with ambient isotopic composition and MSTs from *in vivo* ^{13}C-labelled material for the interpretation of mass spectral fragmentation patterns (Fig. 1). This interpretation effort was based on the detailed EI fragmentation patterns of trimethylsilylated and methoxiaminated carbohydrates (DeJongh et al., 1969; Laine and Sweeley, 1973; MacLeod et al., 2001; Sanz et al., 2002) or amino acids (Abramson et al., 1974; Bergström et al., 1970; Leimer et al., 1977), which have been previously published. Furthermore, interpretation was supported by the mass shifts observed upon *in vivo* ^{13}C-labelling (Fig. 1).

The fragmentation patterns of 58 analytes, comprising approximately 100 electron impact fragments, were analyzed. Representative sugars, organic acids, amino acids, amines and polyols were chosen (cf. Supplementary file 1). This selection represents approximately 7.6% of the current non-redundant Golm Metabolome Database compendium (GMD; Kopka et al., 2005; Schauer et al., 2005a; http://csbdb.mpimp-golm.mpg.de/csbdb/gmd/gmd.html). The sum formula of each mass fragment was deduced from known general fragmentation reactions and available references (see above). For further referencing all obtained fragment information was linked to the mass spectrum identifier system used by GMD (MPIMP-ID). The ^{12}C- and ^{13}C-monoisotopic masses and the respective number of carbon atoms, which originate from the carbon-backbone of each metabolite and are not introduced by chemical derivatization reagents, were empirically determined from ambient and fully *in vivo* labelled MSTs (Fig. 1). In agreement with the GC-EI-TOF-MS instrument specifications, monoisotopic masses are given at full mass unit precision.

Mass fragments comprising the full metabolite carbon-backbone, such as M^+ (molecular ion) or $M-15^+$ (i.e. a mass fragment generated from M through a loss of 15 a.m.u.), were mostly present at low intensities and in some cases below detection limit. Through our effort we now offer alternative fragment ions for mass isotopomer

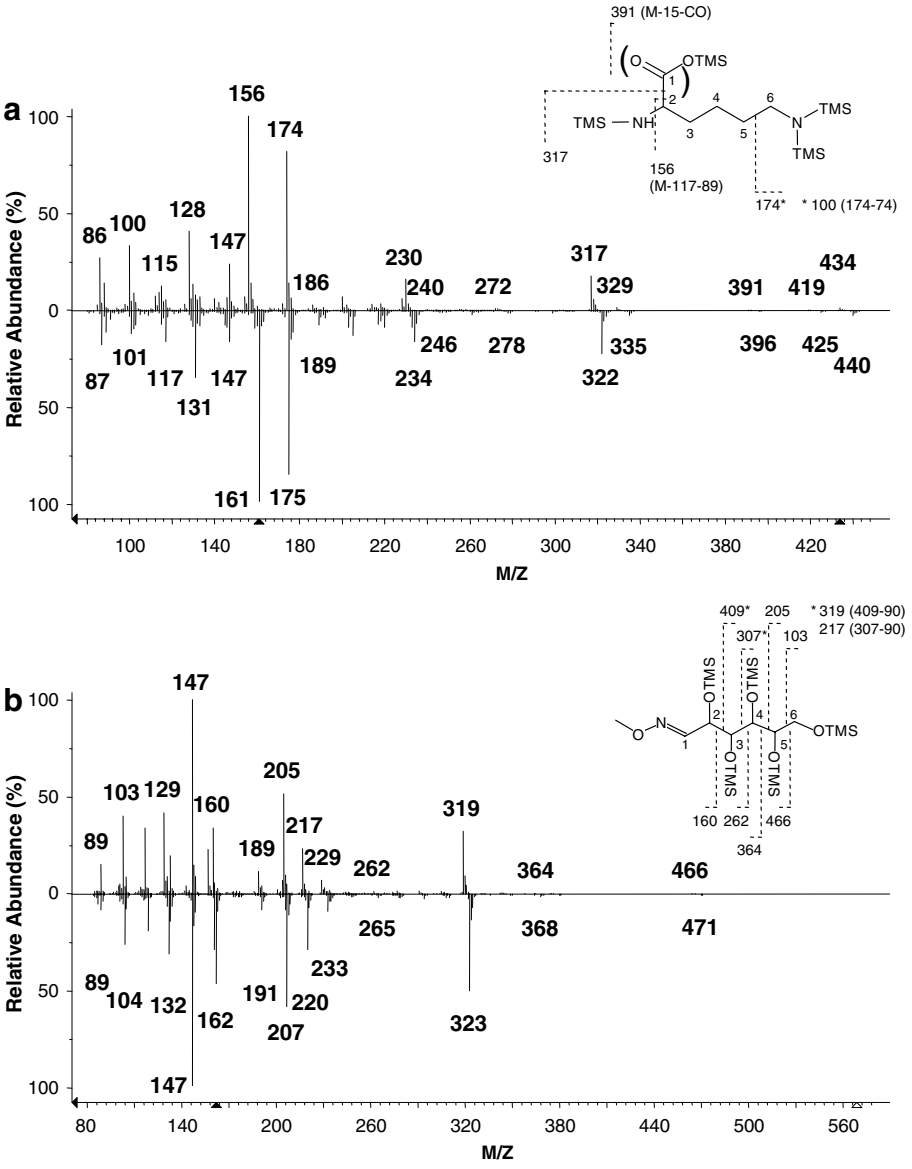

Fig. 1. Representative interpretation of GC-EI-TOF-MS mass spectra of (a) a lysine (4TMS), A192003*, and (b) a hexoaldose analyte, for example glucose (1MEOX) (5TMS), A191001*. Availability of ambient and fully labelled ^{13}C-mass isotopomer specta supported interpretation of known general fragmentation reactions from previous reports. Note (1) the benefit of the methoxyamine chemical tag, which allowed distinction of a $C_1 \rightarrow C_6$ and a $C_6 \rightarrow C_1$ fragment series of reducing sugars. (2) Some fragmentations may be indicative of specific functional moieties and thus useful for functional group mass spectrometry, such as the occurrence of *m/z* 174 → 175, which represents $C_7H_{20}NSi_2^+$, typical of primary amines, or of *m/z* 218 → 220 representing $C_8H_{20}NO_2Si_2^+$ with $C_{1,2}$ of amino acids. * Mass spectrum identifier, MPIMP-ID, as used by the Golm Metabolome Database (GMD; http://csbdb.mpimp-golm.mpg.de/csbdb/gmd/gmd.html, cf. fragmentation details reported within Supplementary file 1). Mass spectra were scaled to the fragment ions, (a) *m/z* 156 → 161 or (b) *m/z* 147, and are displayed head to tail.

analysis. As described previously *tert*-butyldimethylsilylation (e.g. Dauner and Sauer, 2000; Fiehn et al., 2000b; Birkemeyer et al., 2003; Klapa et al., 2003) was successfully assessed as an alternative chemical derivatization strategy to obtain full carbon-backbone information through typically abundant M^+, $M-15^+$, as well as $M-57^+$ fragments. This derivatization method, while perfectly suited for complementary analyses of amines, organic acids and amino acids, was, however, not advisable for the analysis of compounds with multiple vicinal diols, for example saccharides. This derivatization scheme was not further used in this study, because we primarily aimed at highest possible comprehensiveness.

Ample information on mass fragments representing different metabolite substructures was available (Fig. 1). Analytes typically exhibited more than one mass fragment, which was amenable to ^{13}C-isotope dilution analysis. However, in agreement with most MS-based methods of flux estimation, the available substructure information rarely provided sufficient information to extract exact labelling information of each single carbon atom. In contrast multiple mass fragments were typically available, which

characterized complementary scission products or partially overlapping metabolite substructures. In some cases fragmentation reactions allowed assessment of the same metabolite substructure using either different mass fragments of the same analyte, for example *m/z* 307 and the daughter product *m/z* 217, which is generated by neutral loss of C_3H_9SiOH (e.g. Fig. 1b). In other cases mass fragments of alternative derivatization products can be used, for example the two *E/Z*-methoxyamination products of reducing sugars or different silylation products, such as the glycine (2TMS) and glycine (3TMS) products (cf. the information on fragmentation sequence and alternative derivatization products within Supplementary file 1).

Cases of alternative sum formula interpretations could be solved empirically by the ^{13}C-induced mass shift. When possible, we annotated the carbon atoms of the metabolite, which were represented by the observed mass fragments (Supplementary file 1). Furthermore, we indicated those mass fragments, which may originate from different substructures of the same compound. Symmetrical compounds were typical for generating ambiguous substructure information, as were oligomers, such as di- or trisaccharides. Other cases of potentially "non-unique" origin, also indicated in Supplementary file 1, can only be recognized and verified after detailed analysis of positional labelled metabolites (e.g. MacLeod et al., 2001).

Methoxyamination of carbonyl-moieties proved to be highly efficient in simplifying the fragmentation pattern of sugar derivatives and allowed discrimination of two fragmentation series, containing the reduced or non-reduced part of the molecules, respectively (Fig. 1b). Many mass fragments were typical of compound classes. For example *m/z* 160 and 262 are indicative of aldoses. These mass fragments represent $C_{1,2}$ and $C_{1,2,3}$ of the sugar, respectively (Fig. 1a). Amino acids and amines also yielded examples of fragments, which represent specific functional groups. For example, the mass fragment *m/z* 174 shifted to 175 when ^{13}C-labelled. This fragment represents the typical ion $C_7H_{20}NSi_2^+$, which contains C_1 of primary amines. Also the mass fragment *m/z* 218 shifted to 220 when ^{13}C-

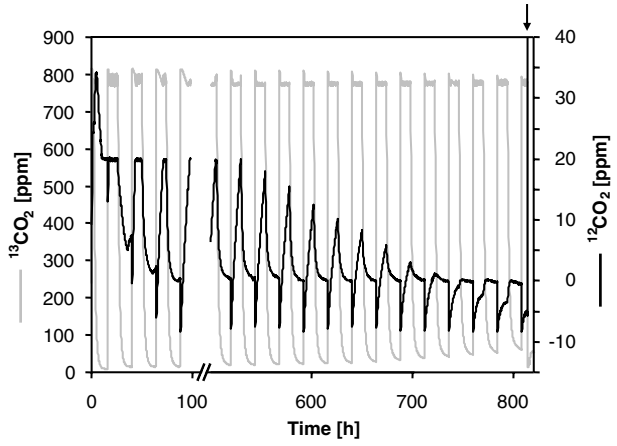

Fig. 2. Saturating $^{13}CO_2$ labelling regime of a population of 60 *Arabidopsis thaliana* Col-0 plants grown in a 6 L hydroponic culture. Plantlets were pre-grown in ambient conditions. At the four-leaf stage a developmentally homogenous population was transferred to $^{13}CO_2$ labelling. The upper $^{12}CO_2$ threshold was set to ~20 ppm during the day; above threshold emitted $^{12}CO_2$ was replaced by $^{13}CO_2$. At night the atmosphere was kept CO_2-free to save $^{13}CO_2$. Growth conditions were a 10 h day at 113.5 (SD = 6.0) μmol m^{-2} s^{-1}, 23.7 (SD = 0.5) °C, 71.8 (SD = 2.4)% relative humidity, 22.3 (SD = 0.3)% O_2, 776.6 (SD = 78.2) ppm total $^{13}CO_2$ and 14 h night at 6.8 (SD = 10.4) μmol m^{-2} s^{-1}, 19.7 (SD = 1.1) °C, 68.7 (SD = 2.0)% relative humidity, 22.3 (SD = 0.3)% O_2, 101.9 (SD = 154.1) ppm total $^{13}CO_2$. In this experiment 1.2 L $^{13}CO_2$ was spent to generate 1.528 g (FW) shoot and 1.796 g (FW) root material. The arrow indicates the start of the isotope dilution experiment. SD indicates standard deviation.

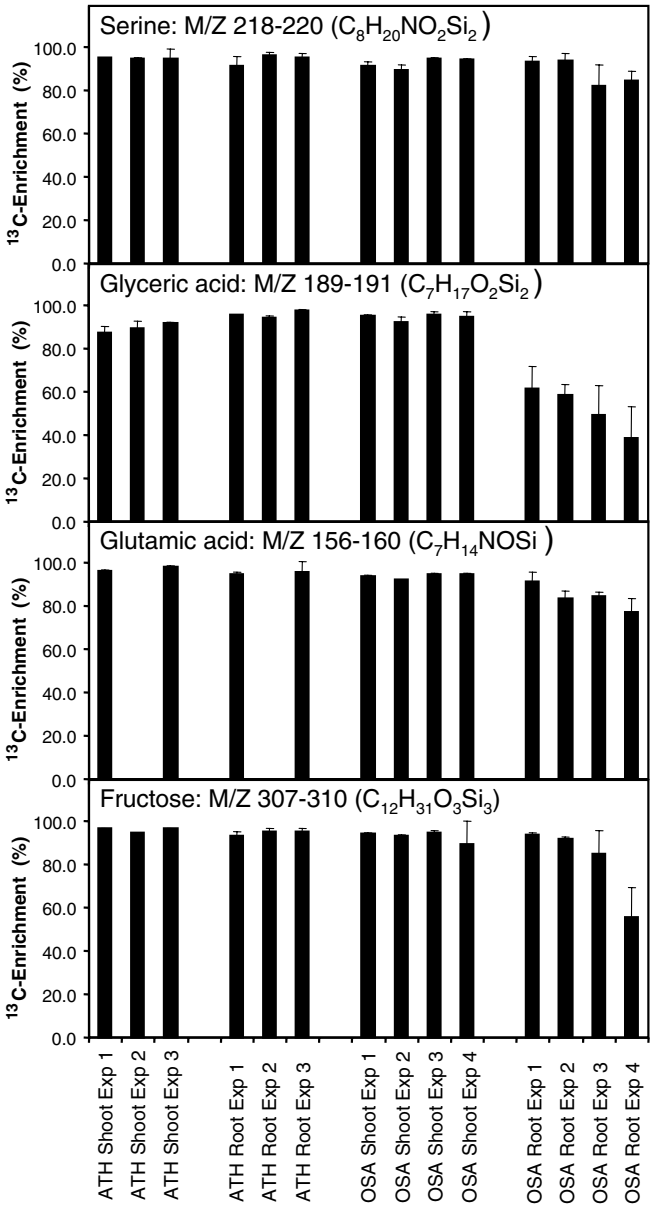

Fig. 3. *In vivo* saturated ^{13}C-isotope enrichment of root and shoot from *Arabidopsis thaliana* Col-0 or *Oryza sativa* plants. Repeatability of serine (A138001), glyceric acid (A135003), glutamic acid (A163001) and fructose (A187002) labelling is demonstrated at the endpoint of ^{13}C-labelling as indicated in Fig. 2. Error bars indicate standard deviation (SD).

labelled. This fragment comprises $C_{1,2}$ of amino acids, namely $C_8H_{20}NO_2Si_2^+$.

The strong EI-induced mass spectral fragmentation of GC-EI analysis may be seen as a drawback for MS-based flux analyses. However, we demonstrated the potential of a detailed analysis of substructures of representative identified metabolites within routine GC-EI-MS profiles. The availability of functional group mass spectrometry (Abramson et al., 1974) ultimately facilitates the first access to the flux analysis of still unknown constituents of metabolite profiles.

The complexity of typical metabolite profiles and the requirement for analysis of multiple mass isotopomers and fragmentation patterns currently limit flux analysis to a subset of the total information, which is routinely available from GC–MS based metabolite profiles. However, the recent introduction of two-dimensional GCxGC-EI-TOF-MS instruments (e.g. Sinha et al., 2004; Kell et al., 2005) will increase the purity of fragment information and thus will extend the application of the method, which is currently implemented and developed in our laboratory using conventional GC-EI-TOF-MS.

2.2. $^{13}CO_2$-labelling of populations of replicate plants

In contrast to microbial flux analyses, which are typically performed in continuous or batch-grown cell cultures, flux studies of higher plants necessitate the use of populations of genetically identical replicated plants. The alternative of subsequent sampling from the same plant bears the risk of concurrent non-controlled wounding reactions and developmental or positional effects. However, monitoring isotope dilution after full $^{13}CO_2$ labelling of the metabolome, as proposed (Birkemeyer et al., 2005), may introduce an additional risk of analytical variability, when compared to conventional flux studies. Therefore, we studied and optimized the ^{13}C-saturated labelling efficiency of metabolite pools. We determined the technical and, even more importantly, the biological plant to plant reproducibility of $^{13}CO_2$-labelling within replicate populations of a hydroponically grown monocotyledon, *Oryza sativa*, and a dicotyledon, *Arabidopsis thaliana*, model species.

2.2.1. Efficiency of $^{13}CO_2$-labelling

The final labelling efficiency per se may not directly influence the accuracy of flux determinations. However, highly repeatable, homogenous labelling of all metabolite pools, ideally in both root and shoot tissue may be deemed prerequisite for optimal and routine experimental reproducibility of studies which exploit the monitoring of isotope dilution after $^{13}CO_2$ labelling. We used the emission of $^{12}CO_2$ during the photoperiod as an indicator for the metabolic ^{13}C-saturation of the plant populations under investigation (Fig. 2). This representative experiment comprised 60 *A. thaliana* Col-0 plants grown in a 6 L hydroponic culture using an airtight and atmospherically controlled growth chamber. Plantlets were at the four-leaf stage when transferred to $^{13}CO_2$-labelling in this enclosed environment. During the initial days plantlets as well as liquid medium contributed to $^{12}CO_2$ generation. To gradually exclude ^{12}C from the system, CO_2 was removed from the enclosed atmosphere using a CO_2 absorber. During the light phase CO_2 was removed and substituted by $^{13}CO_2$-gas, when $^{12}CO_2$ partial pressure increased above 20 ppm. During night CO_2 was completely removed from the atmosphere. The time required for the $^{12}CO_2$ partial pressure to permanently drop below the 20 ppm threshold and finally below detection limit was dependent on the number of plants, developmental stage and species. In the shown *A. thaliana* experiment (Fig. 2) 1.2 L $^{13}CO_2$ was spent to obtain a total of 1.528 g (FW) shoot and 1.796 g (FW) root material. The average ^{13}C-enrichment ± standard deviation (SD), as reproduced in 3 (*A. thaliana*) and 4 (*O. sativa*) independent labelling experiments was 90.2 (±7.3)% and 78.6 (±15.6)% for shoots and roots of *O. sativa* and 91.5 (±10.5)% and 90.2 (±9.7)% for shoots and roots of *A. thaliana*, respectively.

Details of the behaviour of specific mass fragments and best labelling results, approximately 98% (*A. thaliana*) and

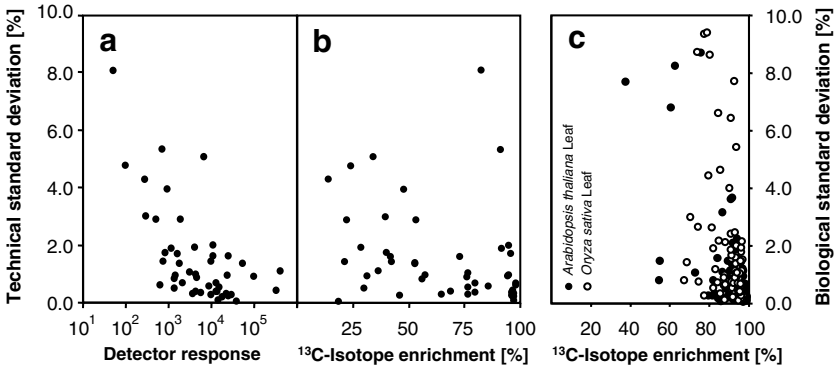

Fig. 4. Influence of (a) detector response, represented as arbitrary ion current, and of (b) ^{13}C-isotope enrichment on the technical standard deviation of ^{13}C-isotope enrichment from complex GC-EI-TOF-MS metabolite profiles of a pool of partially labelled *Arabidopsis thaliana* Col-0 plants. The average standard deviation of 47 representative mass fragments was 1.5% and may increase slightly, when approaching GC-EI-TOF-MS detection limit. (c) The plant to plant standard deviation within a population of simultaneously labelled *Arabidopsis thaliana* Col-0 and *Oryza sativa* plants. Average standard deviation was 1.0% and 1.8%, respectively ($n = 4$–8).

97% (*O. sativa*), may be found in Supplementary file 1. In general the final labelling efficiency was organ and metabolite specific (Fig. 3). The higher efficiency and reproducibility of labelling obtained with *A. thaliana*, especially in roots, is likely caused by the smaller carbon resources of its seed compared to the large carbon resources of the caryopsis of *O. sativa*. Thus, in order to optimize results with *O. sativa*, the residual endosperm was removed from young seedlings. This finding indicates that plant species with large carbon storage capacities within the seed will be less amenable to analysis of isotope dilution after $^{13}CO_2$ labelling, unless the storage organ can be severed early in seedling development or labelled seeds are used. Besides glyceric acid, and fructose (Fig. 3), glycine and trehalose were the most sensitive indicators for incomplete labelling of the root metabolome, in both species.

2.2.2. Homogeneity of $^{13}CO_2$-labelling

The technical error of the determination of ^{13}C-labelling efficiency of metabolite pools, which is inherent to GC-EI-TOF-MS metabolite profiling, was estimated using repeated analyses of the same sample. In order to monitor the broad range of possible labelling efficiencies, the sample was prepared from a pool of partially labelled *A. thaliana* Col-0 plants. Average ^{13}C-enrichment (%) and standard deviation was calculated using approximately 50 mass fragments (Fig. 4a and b). The typical technical standard deviation was 1.8% ^{13}C-enrichment. This technical standard deviation was independent of the degree of ^{13}C-enrichment (Fig. 4b), but clearly dependent on the magnitude of the

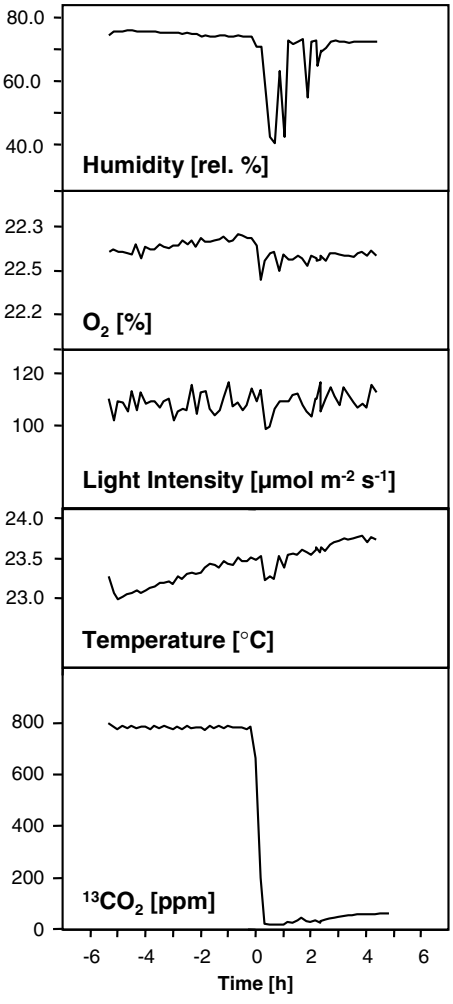

Fig. 5. Homeostasis of environmental conditions during the photoperiod following $^{13}CO_2$ to ambient $^{12}CO_2$ replacement. The parameters were recorded under the conditions of rapid plant sampling, which are required for kinetic studies. Light intensity, temperature and O_2 concentration showed negligible fluctuations. The relative humidity responded to each sampling and the mandatory initial $^{13}CO_2$ flush-out of the growth chamber.

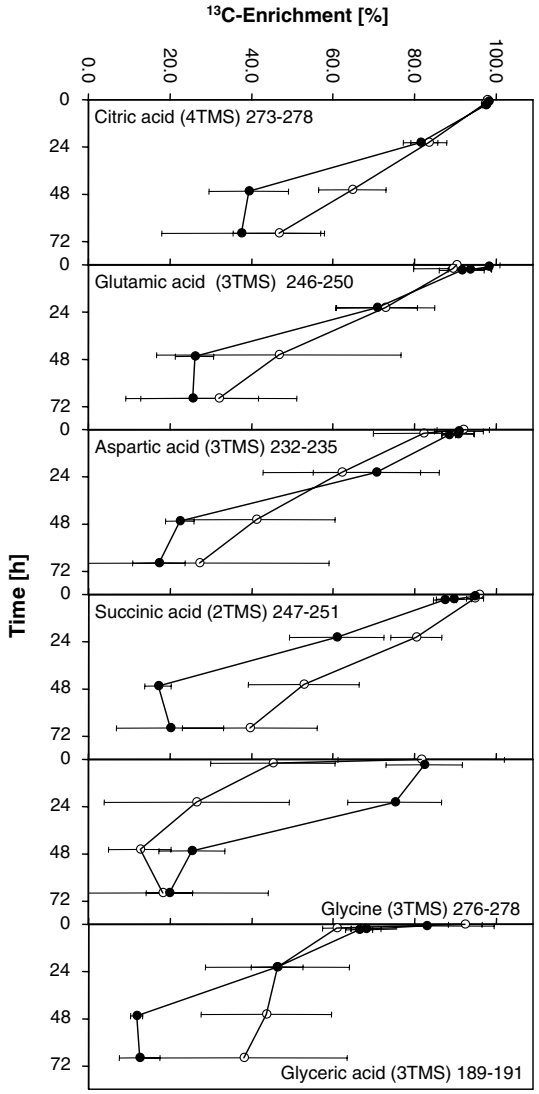

Fig. 6. Long-term kinetics of isotope dilution after $^{13}CO_2$ labelling. Exemplary metabolite pools from *Arabidopsis thaliana* Col-0 shoot (open circles) and root tissue (closed circles) were monitored during a 3 day period following exposure to ambient CO_2. Single plants were analyzed. Plant to plant variation increases dramatically after the first night. Metabolite specific differential behaviour reflecting the shoot to root differences of carbon-partitioning was demonstrated (cf. Table 2, Exp. 1). Error bars indicate standard deviation (SD).

monitored detector response (Fig. 4a). The detection limit of the GC-EI-TOF-MS system used in this study is typically reached at 250–500 arbitrary ion current units with the signal to noise cut-off set to approximately 10.

The "biological" standard deviation calculated from single plant measurements of a simultaneously labelled, genetically homogenous plant population was clearly within the limits of the technical error (Fig. 4c). This result was obtained using shoot material of optimally labelled plant populations. The average standard deviation of all analyzed, maximally labelled mass fragments was 1.0% in shoots and, 2.7% in roots of *A. thaliana*, 1.8% in shoots and 9.0% in roots of *O. sativa*, respectively (Fig. 3 and Supplementary file 1). In conclusion, the full labelling of plants is a prerequisite for optimum experimental homogeneity. Labelling of the root system is subject to higher variability, especially in *O. sativa*. Because *A. thaliana* populations were more amenable to repeatable and homogenous labelling in both organs, we focused on this model in subsequent experiments.

2.3. Assessment of experimental homeostasis during isotope dilution after $^{13}CO_2$ labelling

In plants, the assumption of steady state will be restricted to rare cases. Indeed non-steady state conditions were clearly demonstrated, for example by phenotyping transcriptional, enzymatic, and metabolic changes throughout the diurnal cycle of *A. thaliana* (Blaesing et al., 2005; Gibon et al., 2006). In particular, the first hours after dawn of each photoperiod were shown to yield major changes at all system levels. For this reason we chose to start flux studies in the middle of the photoperiod (Fig. 5). Among a set of selected physico-chemical parameters only the relative humidity could not be kept constant during the initial period of $^{13}CO_2$–$^{12}CO_2$ exchange. All parameters were recorded under conditions of concurrent rapid sampling (Fig. 5). This finding held also true during three subsequent days of extended sampling (data not shown).

The maximum monitoring period, 3 days, was chosen to cover the time required for all metabolite pools to drop below approximately 50% ^{13}C-labelling (Fig. 6). Selected enzyme activities were employed to test for an effect of ^{13}C–^{12}C-substitution during that period. We did not detect a significant impact of ^{12}C-enrichment on enzyme activities during short and extended monitoring periods (Table 1). This might be due to the low protein turnover as compared to metabolic turnover and/or by the fact that ^{13}C-labelled enzymes might retain the same enzymatic properties as ^{12}C-labelled enzymes. We interpret our finding as a first indication that the monitoring of isotope dilution after $^{13}CO_2$ labelling is not impaired by major changes in enzyme kinetic properties.

2.4. Long-term isotope dilution experiments

Metabolite pools have highly diverse ^{13}C-half-life and kinetic behaviour (Fig. 6). The characteristics of isotope dilution kinetics during an extended monitoring period demonstrated clear differences between the metabolite pools of root compared to shoot (Fig. 6). As expected, metabolites linked to respiratory processes, such as citric, malic (data not shown), and succinic acid exhibited a stronger long-term carbon-partitioning into roots. Surprisingly, glyceric acid exhibited a similar pattern, suggesting that this metabolite was also actively metabolized in roots. In contrast, shoots exhibited a preferential carbon-partitioning into glycine and serine (data no shown), most likely due to photorespiration. The long-term kinetic behaviour of isotope dilution in most root pools was equal or even faster compared to shoot pools. Aspartic acid and glycine pools, exhibited a perceptible delay compared to the kinetic behaviour observed in leaves. In some cases, the time course of isotope dilution was found to be biphasic. For example, during the first photoperiod, the incorporation

Table 1
Effect of ambient CO_2 incorporation into ^{13}C-saturated *Arabidopsis thaliana* Col-0 plants on selected enzyme activities

Enzyme		Experiment 1			Experiment 2					
		Day 0			Day 0 [+1.5 h]		Day 2 [±3.5 h]		Day 3 [±3.5 h]	
		Activity [nmol min^{-1} g^{-1} (FW)]	SD	*n*	Fold change	*p*	Fold change	*p*	Fold change	*p*
Isocitrate dehydrogenase (NAD+)	EC 1.1.1.41	88.9	18.5	9	1.00	0.981	0.88	0.441	0.71	0.058
Glycerate kinase	EC 2.7.1.31	2399.5	1576.6	10	1.05	0.898	1.07	0.831	1.27	0.493
Phosphoglycerate kinase	EC 2.7.2.3	37824.9	19332.0	10	1.18	0.520	1.14	0.581	1.22	0.420
Transketolase	EC 2.2.1.1	2186.7	839.9	10	1.25	0.264	1.18	0.408	1.18	0.452

Pools of rosette leaves (shoot) were exposed to ambient CO_2 at 4 h after dawn and sampled between 0 and 1.5 h on day 0 or ±3.5 h on subsequent days. Exemplary enzyme activities were analyzed according to Gibon et al. (2004). Activities of isocitrate dehydrogenase (NAD^+) EC 1.1.1.41, glycerate kinase EC 2.7.1.31, phosphoglycerate kinase EC 2.7.2.3, and transketolase EC 2.2.1.1 did not exhibit significant changes upon *in vivo* ^{12}C–^{13}C-isotope exchange neither between independent experiments nor up to 3 days after exposure to ambient CO_2.

into both aspartic and glyceric acid was initially fast, but then slowed down dramatically (Fig. 6).

Not unexpectedly we observed an increasing experimental variability within populations of replicate plants from day to day (Fig. 6). We subsequently focused on the first two photoperiods for a better resolution of the initial dilution kinetics and an improved characterization of the increasing plant to plant variability.

2.5. Short-term isotope dilution experiments

Short-term isotope dilution confirmed the high diversity of ^{13}C-half-life observed in different metabolite pools. In addition, the initial dilution kinetic was apparently linear and shifted subsequently to an asymptotic behaviour (Fig. 7). Unexpectedly, the asymptotic ^{13}C-decay was metabolite dependent and none of the metabolite pools approximated ambient ^{13}C-enrichment. Two parallel processes may apply. (1) Newly assimilated carbon competes with carbon derived from internal stores and an equilibrium phase is reached after the initial linear dilution phase. In other words metabolite pools may reach a quasi steady state after different times. (2) Additionally, in plant cells most metabolites are present in two or more pools, which exhibit slow exchange rates. Furthermore one of these pools would be required to behave metabolically inert, for example the vacuole or possibly the apoplast, whereas the others may represent metabolically highly active pools, such as plastid, mitochondria or cytosol.

Despite the high variability observed during extended monitoring, we were able to accurately monitor isotope dilution by sampling single plants in 1–5 min intervals during the first photoperiod (Fig. 7). Thus initial dilution kinetics can be obtained for metabolites with a fast ^{13}C-half-life, like glyceric acid, sucrose, and fructose. However, sampling needs to remain equally spaced throughout the whole monitoring period because of the high diversity of metabolite ^{13}C-half-life (cf. sucrose, succinic or fumaric acid in Fig. 7). For improved monitoring of metabolites with low ^{13}C-half-life, extension of measurements towards the end of the first photoperiod is advised. Extended monitoring into the second photoperiod showed drastic increase of plant to plant variability. This effect subsequently superseded and thus obscured the kinetic behaviour (insert of Fig. 7). Therefore extension towards 1 day monitoring may only be done for metabolite pools with extremely high ^{13}C-half-life.

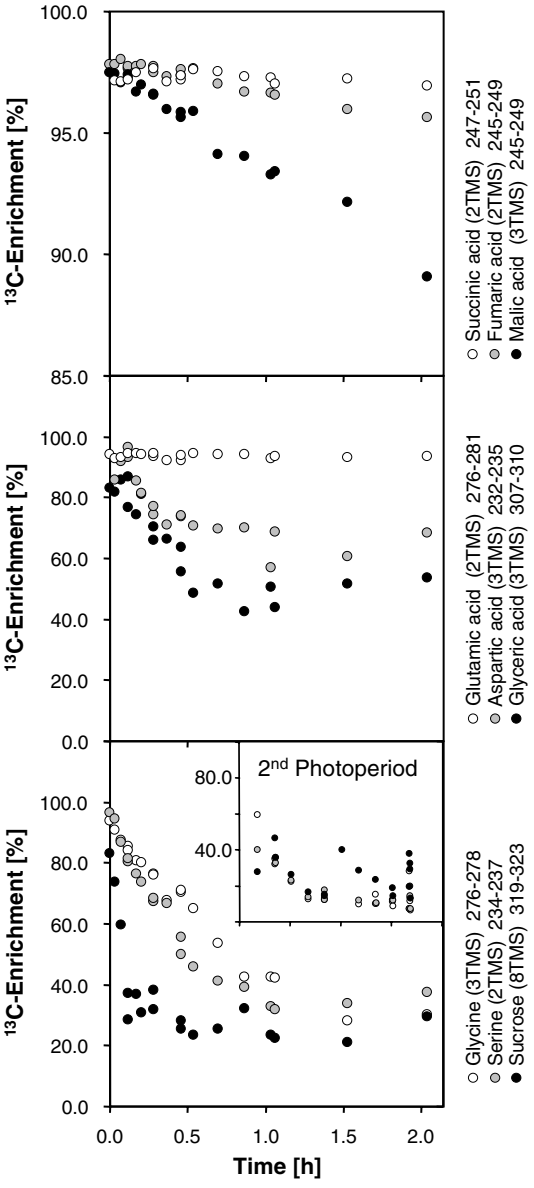

Fig. 7. The short-term kinetic behaviour of ^{13}C-isotope dilution into exemplary metabolite pools of *Arabidopsis thaliana* Col-0 shoot upon exposure to ambient CO_2 (cf. Table 2, Exp. 4). ^{13}C-decay was traced within the initial 2 h of the first light period and throughout the second photoperiod (insert).

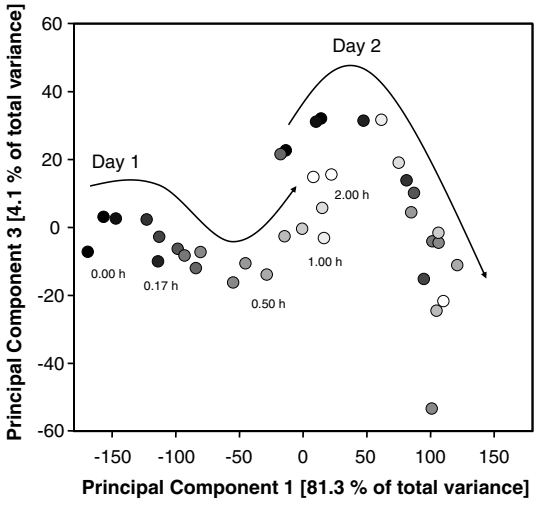

Fig. 8. Principal component analysis of ^{13}C-isotope enrichment kinetics of metabolite pools from *Arabidopsis thaliana* Col-0 shoot upon exposure to ambient CO_2. The temporal sequence of sampling is indicated per day by grey scale. A subset of the metabolites, which show high contribution to the first component of this analysis, is shown in Fig. 7.

2.6. Analysis of the ^{13}C-isotope decay phenotype

We applied principal component analysis (PCA) to analyse the increase in plant to plant variability between the first and second photoperiod (Fig. 8). We focussed on shoot samples of *A. thaliana* and thus avoided obvious variances caused by species and organ differences. Accessing the major variance from a 28 h time course of experiment 4 (Fig. 7 and Table 2), we tested, whether plants of the second photoperiod might follow a common kinetic behaviour despite high apparent variability. All samples appeared to follow the same isotope dilution kinetic during the first and the second day, as was indicated by the first principal component, which comprised 81.3% of the total variance. Interestingly, samples received a slight off-set during the intervening night period. We reason that this observation can be explained by utilization of stored ^{13}C during the night. A non-linear behaviour was characterized by the 3rd principal component (4.1% of the total variance). This effect was intensified on the second day compared to first. The 2nd (neglected) principal component comprised 4.5% of the total variance. This part of the variance in the data set could not be interpreted using the known sample classifications of our experimental design.

As expected the sequence of samples, which was revealed by PCA analysis, was clearly in agreement with the time of sampling during the first day. During the second day, the time of sampling allowed only a rough prediction of the respective kinetic metabolic phenotype (Fig. 8). Nevertheless, by visual inspection all samples appeared to exhibit a common behaviour.

We hypothesized that the apparent off-set during the intervening night period may be the source of variability. During night plants not only utilize the ^{12}C-starch generated in the previous photoperiod but may also mobilize long-term ^{13}C-carbon resources, when starch is depleted. If this competition of resources is variable in individual plants, a parameter, which is indicative of the assimilated CO_2 within the soluble metabolite pools, may be applied for correction. We tested this assumption by calculation of the mean ^{13}C-enrichment from all mass fragments. Compared to the sampling time, the mean enrichment exhibited a better fit to the sequence of samples obtained by PCA analysis (cf. graphical abstract).

Table 2
Assessment of reaction order assumptions for the ^{13}C-half-life calculation of metabolite pools after short and extended periods of $^{13}CO_2$-isotope dilution

Experiment	Organ	Observation period (h)	0. Order assumption		1. Order assumption		2. Order assumption		3. Order assumption	
			r^2	p	r^2	p	r^2	p	r^2	p
Glycine (3TMS) 174–175										
Exp. 1	Leaf	72	0.494	5.5E−04	0.614	4.4E−05	0.615	4.2E−05	0.554	1.7E−04
Exp. 1	Root	72	0.582	1.5E−03	0.691	2.3E−04	0.578	1.6E−03	0.395	1.6E−02
Exp. 2	Leaf	48	0.712	4.3E−03	0.720	3.8E−03	0.624	1.1E−02	0.539	2.4E−02
Exp. 3	Leaf	28	0.801	2.6E−11	0.780	1.1E−10	0.589	7.5E−07	0.457	4.1E−05
Exp. 4	Leaf	28	0.584	1.3E−10	0.661	1.8E−12	0.621	1.9E−11	0.523	2.7E−09
Exp. 4*	Leaf	2	0.900	1.4E−11	**0.940**	1.5E−13	**0.939**	1.7E−13	0.895	2.0E−11
Glyceric acid (3TMS) 189–191										
Exp. 1	Leaf	72	0.494	5.5E−04	0.614	4.4E−05	0.615	4.2E−05	0.554	1.7E−04
Exp. 1	Leaf	72	0.422	1.1E−03	0.356	3.4E−03	0.233	2.3E−02	0.139	8.7E−02
Exp. 1	Root	72	0.973	4.1E−05	0.906	9.4E−04	0.793	7.2E−03	0.690	2.1E−02
Exp. 2	Leaf	48	0.512	3.0E−02	0.601	1.4E−02	0.615	1.2E−02	0.593	1.5E−02
Exp. 3	Leaf	28	0.583	9.1E−07	0.586	8.2E−07	0.526	5.9E−06	0.447	5.3E−05
Exp. 4	Leaf	28	0.449	5.8E−06	0.463	3.6E−06	0.434	9.3E−06	0.370	6.5E−05
Exp. 4*	Leaf	2	**0.521**	4.8E−04	**0.507**	6.3E−04	0.478	1.0E−03	0.438	2.0E−03
Malic acid (3TMS) 245–249										
Exp. 1	Leaf	72	0.671	3.2E−06	0.589	3.1E−05	0.494	2.7E−04	0.404	1.5E−03
Exp. 1	Root	72	0.887	1.9E−07	0.841	1.4E−06	0.719	4.7E−05	0.569	8.2E−04
Exp. 2	Leaf	48	0.839	5.2E−04	0.818	8.1E−04	0.731	3.3E−03	0.595	1.5E−02
Exp. 3	Leaf	28	0.726	2.3E−09	0.635	1.4E−07	0.547	3.0E−06	0.478	2.3E−05
Exp. 4	Leaf	28	0.690	2.1E−10	0.621	7.0E−09	0.542	2.0E−07	0.458	4.3E−06
Exp. 4*	Leaf	2	**0.982**	3.1E−16	**0.981**	3.9E−16	**0.980**	5.8E−16	**0.979**	1.0E−15
Fructose (1MEOX) (5TMS) 307–310										
Exp. 1	Leaf	72	n.d.		n.d.		n.d.		n.d.	
Exp. 1	Root	72	0.715	5.3E−04	0.826	4.2E−05	0.697	7.2E−04	0.471	1.4E−02
Exp. 2	Leaf	48	0.691	5.5E−03	0.708	4.4E−03	0.530	2.6E−02	0.383	7.5E−02
Exp. 3	Leaf	28	0.673	2.9E−08	0.504	1.1E−05	0.310	1.4E−03	0.197	1.4E−02
Exp. 4	Leaf	28	0.023	3.7E−01	0.025	3.5E−01	0.026	3.4E−01	0.024	3.6E−01
Exp. 4*	Leaf	2	0.594	1.1E−04	**0.676**	1.6E−05	**0.684**	1.3E−05	0.614	7.3E−05

Linear fit of a 0, 1st, 2nd, and 3rd reaction order assumption was tested by correlation coefficient (r^2) and significance (p). Representative metabolites are shown and optimum results of short-term monitoring indicated bold (n.d., not determined). Data are from four independent experiments, Exp. 1–4. Exp. 4* represents the 2 h subset of Exp. 4.

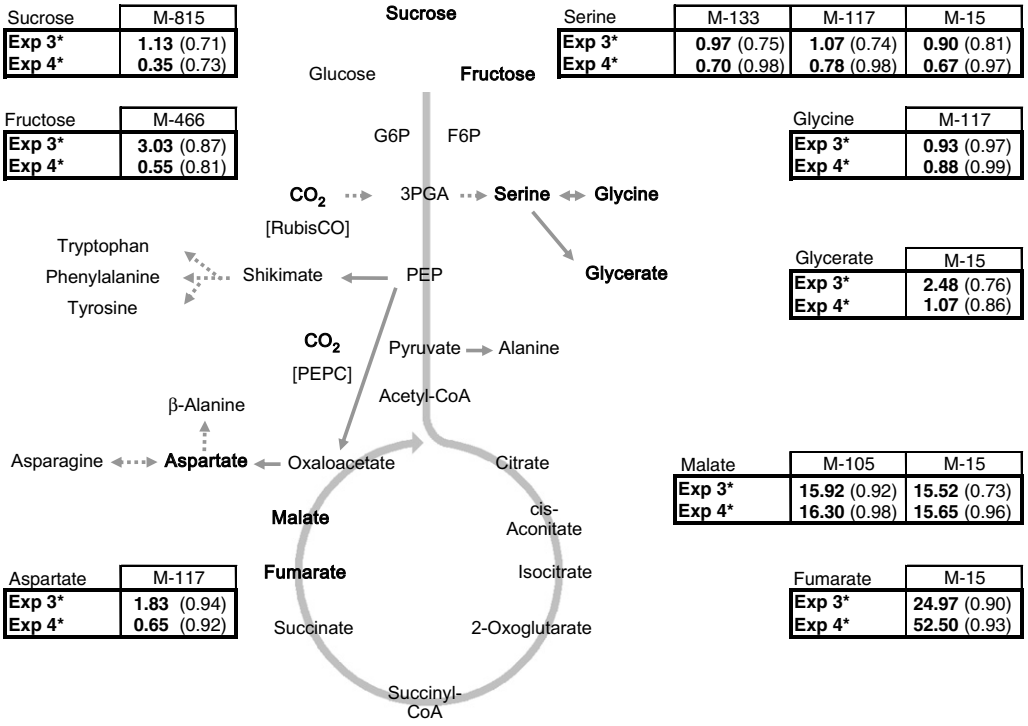

Fig. 9. Estimation of ^{13}C-half-life in metabolite pools of *Arabidopsis thaliana* shoots using a 2 h kinetic monitoring period. Experimental repeatability is indicated using the short-term results of two independent experiments, namely Exp. 3 and 4 (cf. Table 2). Exemplary results using alternative mass fragments of selected metabolite derivatives are shown. Half-life is expressed in decimal hour format and the respective regression coefficient, r^2, is reported in brackets.

Even though detailed kinetic analysis appeared to be impaired from the second photoperiod onwards we concluded, that data normalization using an indicator of total *de novo* carbon assimilation may alleviate the restriction to one photoperiod. This aspect was, however, not further investigated in the course of this study.

2.7. Estimation of the ^{13}C-half-life of metabolite pools

The development of suitable mathematical models for the presented empirical observation of ^{13}C-dilution kinetics and carbon-partitioning in higher plants is not a trivial task. As a first and strongly simplifying approach we assessed the calculation of ^{13}C-half-life of metabolite pools. Half-life calculations require assumption of reaction order. We tested 0, 1st, 2nd, and 3rd reaction order assumptions on both short-term (up to 2 h) and extended (up to 3 days) monitoring of isotope dilution after $^{13}CO_2$ labelling (Table 2). The choice of reaction order had a small effect on the quality of linear fit as determined by correlation coefficient and significance. In most cases, the 1st reaction order assumption was slightly superior and was therefore used. The analysis demonstrated that half-life calculation is indeed a simplification and may fail in some experiments or for single metabolites (cf. fructose in experiment 4; Table 2). Furthermore, the quality of fit was time course- and organ-dependent, for example glyceric acid in experiment 1 (Table 2).

Using the half-life parameter, we tested the experimental repeatability of short-term kinetic results in two independent experiments (Fig. 9). A good repeatability was found for most metabolites and ^{13}C-half-life ranging between 20 min and more than 52 h were detected. Nevertheless, we observed variability between experiments, for example sucrose and fructose (Fig. 9), which may result from slight environmental or seasonal changes. As a consequence the use of a reference genotype and highly standardized growth conditions is indicated for future comparative studies (see below).

3. Concluding remarks

We demonstrated the potential of routine GC-EI-TOF-MS profiling for flux analysis and provided an initial set of mass fragments to monitor flux and isotope dilution experiments. This set of mass fragments allows access to the steady state, but more importantly to the transient kinetics of isotope dilution at few defined carbon positions and many substructures of the targeted metabolites. Positional information can typically only be obtained by NMR studies but not through mass isotopomer analyses of molecular ions. Compared to NMR analyses the information from GC-EI-TOF-MS fragment analyses will always be limited. Only part of the carbon positions or substructures will be accessible due to the limitations of the fragmentation reac-

tions. In addition, not all mass fragment observations can be exploited, because of frequent co-elution of compounds in complex mixtures. An extension and refinement of the method can be expected, especially through improved separation of complex mixtures using GC×GC-EI-TOF-MS. The method in general will continuously benefit from the synergy with the technical advances made in GC-EI-TOF-MS metabolite profiling technology, specifically the continued substance and fragment elucidation process.

The current major limitation of our method is the lack of information on the metabolic pool sizes. The half-life of ^{13}C-label in metabolic pools is dependent on the respective pool sizes. Metabolite concentrations differ for example in response to diurnal changes. Using the sum of all mass isotopomers, which represent a fragment or molecular ion, we were able to detect relative concentration changes during the time courses we recorded in our experiments (data not shown). The estimation of exact metabolite concentrations at each time point and from each plant is a clear necessity for the improved interpretation of our primary data, as metabolite pools typically change between, species, genotypes, individuals and environmental conditions. Quantification of GC–MS analyses is routinely performed using external calibration and will be included in our future experiments. The underlying assessment of metabolite recovery, linear range and quantification using GC–MS based metabolite profiling has been reported previously (e.g. Roessner et al., 2001; Roessner-Tunali et al., 2003; Schauer et al., 2005b).

The use of populations of genetically identical, replicate plants for flux analyses was assessed. We demonstrated that the monitoring of isotope dilution after $^{13}CO_2$ labelling is feasible and that the initial variability of the plant population can be adjusted to be within the technical error of the analytic GC–MS system. However, accurate kinetic measurements are currently restricted to the initial monitoring hours. With a clear understanding of the potential and current limitations of the method mentioned above, we now head towards a phenotyping tool, which may be suitable for the estimation of carbon-partitioning into a range of representative shoot and root pools of model plant species. We suggest that the analysis of genetically modified or mutant plants may be feasible using a pair wise comparative experimental design with mixed populations of two genotypes, namely a reference genotype such as *A. thaliana* Col-0 and the genotype of interest. Both genotypes will be simultaneously grown, labelled by $^{13}CO_2$, and sampled after initiation of isotope dilution. In analogy to the concept of metabolite profiling (Fiehn et al., 2000a; Roessner et al., 2000) we envision that the half-life of ^{13}C-label in the monitored metabolic pools can be expressed as a relative change compared to the reference genotype. Thus the reference genotype will ensure comparability between independent experiments. In a similar design the adaptation of plants to physico-chemical or nutrient stresses may be feasible by simultaneous cultivation and monitoring of isotope dilution after $^{13}CO_2$ labelling of one genotype under standardized and in parallel under modified hydroponic conditions.

The presented numerical analysis of our empirical data is still in its infancy. Half-life calculations of isotope dilution after $^{13}CO_2$ labelling represent only a first, roughly simplifying approach of data reduction. We currently neglect the possibility of non-homogenous labelling and potential means to correct for the plant to plant variability. In addition the transient labelling kinetics of the different mass isotopomers, which may deviate from the expected homogenous isotope dilution behaviour, remains unexplored.

We are intrigued by our observation of quasi steady states, which do not approach the ambient input $^{12}C/^{13}C$ ratio in several subsequent photoperiods. This finding might be characteristic for whole organ analysis of higher plants and may be explained by the presence of large ''inert pools'' of metabolites, e.g. in the vacuole, which we currently do not separate from metabolically more active subcellular pools. In an alternative, but not mutually exclusive scenario previously assimilated carbon may compete with de novo assimilation. These current assumptions need to be experimentally analyzed prior to future modelling approaches.

4. Experimental

4.1. Chemicals and plants

The seeds of the model plant, *O. sativa* L. IR57111, were obtained from the International Rice Research Institute (IRRI; Los Baños, Philippines). *A. thaliana* L. Columbia-0 (Col-0) was a gift from Prof. T. Altmann (University of Potsdam, Germany).

Carbon dioxide (CO_2, isotopic purity 99 atom% ^{13}C, <3 atom% ^{18}O) was purchased from Sigma–Aldrich (Steinheim, Germany). All other chemicals were obtained from the same company and of highest available purity.

4.2. GC-EI-TOF-MS profiling analysis

Complete shoot material of *O. sativa* and of *A. thaliana* (rosette leaves) was sampled. Root material was taken from hydroponic culture, rinsed under tap water and soaked dry on filter paper. Metabolic inactivation was by shock freezing in liquid nitrogen. Time until frozen was 15–45 s. Metabolite extraction and chemical derivatization, namely methoxyamination and subsequent trimethylsilylation was as initially suggested by Fiehn et al. (2000a) and Roessner et al. (2000). GC-EI-TOF-MS profiling was performed using a FactorFour VF-5 ms capillary column, 30 m length, 0.25 mm inner diameter, 0.25 μm film thickness with a 10 m EZ-guard pre-column (Varian BV, Middelburg, Netherlands), and an Agilent 6890N gas chromatograph with splitless injection and electronic pressure control (Agilent, Böblingen, Germany) mounted to a Pegasus III time-of-flight

mass spectrometer (LECO Instrumente GmbH, Mönchengladbach, Germany). The initial method was slightly modified and adapted for automated GC-EI-TOF-MS analysis of 30–60 mg (FW) plant material (Wagner et al., 2003; Erban et al., 2006). Metabolites were quantified after mass spectral deconvolution (ChromaTOF software version 1.00, Pegasus driver 1.61, LECO, St. Joseph, MI, USA). The peak height representing arbitrary mass spectral ion currents of each mass isotopomer was used for subsequent numerical analysis. Mass fragment identification and retrieval of respective mass isotopomer distributions was manually supervised.

4.3. GC-EI-TOF-MS compound identification

Metabolites were identified using the NIST05 mass spectral search and comparison software (National Institute of Standards and Technology, Gaithersburg, MD, USA; http://www.nist.gov/srd/mslist.htm) and the mass spectral and retention time index (RI) collection (Schauer et al., 2005a) of the Golm Metabolome Database (GMD; Kopka et al., 2005). Only mass spectra of concurrently analyzed non-labelled plant reference material from root of the respective plant species was used for mass spectral matching. During experimentation an authenticated set of fully labelled ^{13}C-mass spectra was obtained, which was used to crosscheck identification using samples, which were fully ^{13}C-labelled. Automated mass spectral matching was manually supervised and matches accepted with thresholds set to match factor >650 (with maximum match equal to 1000) and RI deviation <1.0%. Information on the chemical derivatives and mass spectra reported in this study, may be found at http://csbdb.mpimp-golm.mpg.de/csbdb/gmd/msri/gmd_smq.html, using the indicated mass spectral identifiers (MPIMP-ID; cf. Supplementary file 1).

4.4. Methods for the maximum $^{13}CO_2$-labelling of plants

Arabidopsis thaliana Col-0 seeds were sterilized by 10 min exposure to 70% ethanol, stratification was 2–3 days at 4 °C. Seed were germinated and pre-grown on 0.75–0.80% Noble Agar with 0.5-fold concentrated hydroponic medium (Gibeaut et al., 1997) using micro-centrifuge tubes. After one week the bottoms of the micro-centrifuge tubes were cut off and fixed onto hydroponic medium. For the following two weeks plants were grown under ambient CO_2 conditions in an 8-h day at 20 °C/18 °C (day/night) air temperature, 60–75% humidity, 120–180 μmol (photons) m^{-2} s^{-1}. At approximately the four-leaf stage, a developmentally homogenous population of up to 60 single plants was transferred with freshly prepared and degassed hydroponic solution to an atmospherically controlled, airtight 40 L growth chamber, in the following called biobox (GMS Gaswechsel-Messsysteme GmbH, Berlin, Germany). The biobox was customized for isotope specific $^{12}CO_2$ and $^{13}CO_2$ measurement and control at ambient or elevated atmospheric pressure. Monitoring options for O_2, atmospheric pressure, temperature, light intensity and relative humidity measurements were available. The set points for growth of *A. thaliana* were 10 h/14 h short day with 23 °C/18 °C air temperature, 19 °C/14 °C dew point temperature, maximum light intensity 150 μmol m^{-2} s^{-1}. The internal atmospheric pressure was dynamically kept 20 mbar above ambient. The controlled atmospheric composition was 21% oxygen and total CO_2 partial pressure set to 800 ppm. During $^{13}CO_2$-labelling a 20 ppm maximum $^{12}CO_2$-threshold was set. Above threshold a non-selective CO_2-absorption trap was used to remove emitted $^{12}CO_2$ in the light period. During night the CO_2-absorption trap was used to remove all atmospheric CO_2 from the biobox to deplete the system of $^{12}CO_2$ released by respiration (Fig. 2; cf. legend to Fig. 5 for data on the level of environmental parameter control). Isotope dilution after $^{13}CO_2$ labelling was achieved by exposure of the growth chamber to the ambient atmosphere and initial manual venting. The CO_2-isotope control settings were reversed and internal air ventilation required for the maintenance of temperature and light settings were found to be sufficient for the subsequent sampling period. The total time required for one experiment including pre-growth of a population of 60 plantlets was 45–50 days with approximately 33–35 days required for full initial labelling (e.g. Fig. 2).

Oryza sativa L. IR57111 was germinated four days in the dark at 28 °C. The germinated embryo was removed from the caryopsis and fixed to a solid lattice with the root submerged in hydroponic medium (Yang et al., 1994). Generation of developmentally homogenous populations of manipulated rice seedling required thorough preparative expertise. The growth conditions of *O. sativa* were modified to 12 h/12 h equal day and night length with constant 26 °C air temperature, 22 °C dew point temperature and maximum light intensity set to 290 μmol m^{-2} s^{-1}. All other conditions were similar to the experimental settings for *A. thaliana*. In this study two potential heterotrophic carbon sources, namely the agar and 1.0 mM (Yang et al., 1994) or 0.07 mM (Gibeaut et al., 1997) ethylenediaminetetraacetate, were neglected.

4.5. Enzyme activities

Enzyme extracts were sampled throughout four photoperiods following the start of isotope dilution after $^{13}CO_2$ labelling and prepared as described previously (Gibon et al., 2004), except 1% Triton-X100 and 20% glycerol were used. Transketolase activity was determined as described by Gibon et al. (2004). Isocitrate dehydrogenase (NAD+) was assayed by 40 min incubation of crude extract or NADH standard in freshly prepared medium comprising 5 mM $MgSO_4$, 1 mM NAD^+ (Roche), 1 mM isocitrate (Sigma–Aldrich) in 50 mM MOPS buffer, pH 7.5. The reaction mixture was stopped by an equal volume of 0.5 M NaOH. After neutralization, NADH produced by isocitrate dehydrogenase (NAD^+) was determined by using

the previously described NAD^+-based cycling protocol (Gibon et al., 2004).

Phosphoglycerate kinase was assayed by 20 min incubation of crude extract or dihydroxyacetone phosphate (Sigma–Aldrich) standard in freshly prepared medium containing 5 mM ATP (Roche), 4 mM 3-phosphoglycerate (Sigma–Aldrich), 1 U triose phosphate isomerase (Roche), 1 U NAD-glyceraldehyde-3-phosphate dehydrogenase (Roche), 2 U glycerol-3-phosphate dehydrogenase (Roche), 5 mM DTT (Sigma–Aldrich), 0.3 mM NADH (Roche), 20 mM $MgCl_2$, 50 mM KCl, 2 mM EDTA, 0.05% Triton-X100 in 100 mM Tricine/KOH, pH 8. The reaction mixture was stopped by an equal volume of 0.5 M HCl in 100 mM Tricine/KOH. After neutralization, generated glycerol-3-phosphate was determined as described (Gibon et al., 2004).

Glycerate kinase was assayed by 20 min incubation of crude extract or 3-phosphoglycerate standard in freshly prepared medium containing 10 mM $MgCl_2$, 0.05% Triton-X100, 5 mM ATP, 2 mM glycerate in 100 mM Tricine/KOH, pH 8. The reaction mixture was stopped by an equal volume 0.5 M HCl in 100 mM Tricine/KOH. After 10 min at room temperature, the solution was neutralized by 0.5 M NaOH. Then generated 3-phosphoglycerate was determined spectrophotometrically at $\lambda = 340$ nm by adding an equal volume of 4 mM $MgCl_2$, 1 U triose-phosphate isomerase (Roche), 10 U phosphoglycerate kinase (Sigma), 2 U glycerol-3-phosphate dehydrogenase (Roche), 1 U NAD-glyceraldehyde-3-phosphate dehydrogenase (Roche), 5 U glycerol-3-phosphate oxidase (Roche), 10 mM ATP (Roche), and 1 mM NADH in 100 mM Tricine/KOH, pH 8.

4.6. Calculations

Standard deviation was used throughout the manuscript to characterize experimental variability. PCA was performed as described earlier using ^{13}C-enrichment instead of the logarithm of normalized response ratios, which is typically used for metabolite profile analysis (e.g. Desbrosses et al., 2005).

^{13}C-enrichment was calculated from manually retrieved and validated mass isotopomer distributions of identified and characterized EI-induced mass fragments. Apparent ^{13}C-enrichment was corrected for the bias introduced by naturally occurring stable mass isotopes of other elements or of carbon atoms, which were introduced by chemical derivatization, using infinite dimensional matrix calculus (Wahl et al., 2004) provided by the software package of the authors. This software required a MatLab (The MathWorks, Natick, USA) programming environment. Alternatively we used a more conventional subtractive method, which corrects for natural isotope abundances (e.g. Fernandez et al., 1996). Both methods yielded highly similar correction results. The difference between both correction schemes was smaller than the contribution of the technical error, which was inherent to GC-EI-TOF-MS metabolite profiling. Data management, data transformation, basic calculations and regression analysis were performed using Microsoft Office Excel 2003 options.

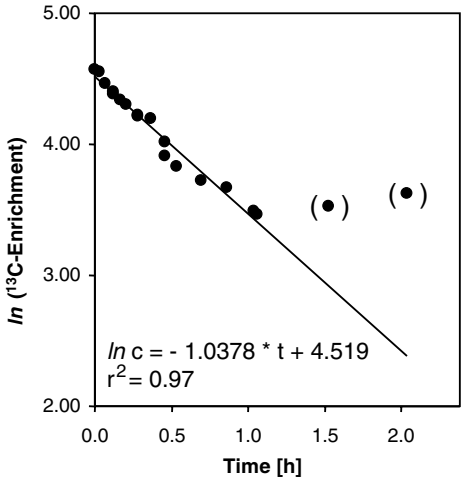

Fig. 10. Exemplary estimation of the half-life of ^{13}C-label in the serine pool using the serine (2TMS) 234–237 data shown in Fig. 7. The resulting ^{13}C-half-life is shown in Fig. 9 (serine, M-15, Exp. 4*). Empirically determined ^{13}C-enrichment was *ln*-transformed and subjected to linear regression after outlier removal. Removed measurements are indicated by brackets.

Half-life calculation was performed using the equation

$$\ln c = -k * t + \ln c_0,$$

where c represents the corrected ^{13}C-enrichment (%) and t equals time after start of isotope dilution (h). Half-life, $t_{1/2}$, was calculated from the rate constant k according to $t_{1/2} = \ln 2 * k^{-1}$. Empirical data were fitted to the above integrated rate equation by linear regression after removal of outliers (e.g. Fig. 10).

Acknowledgements

The authors acknowledge the long standing support and encouragement by Prof. L. Willmitzer and Prof. M. Stitt, Max Planck Institute of Molecular Plant Physiology, Am Muehlenberg 1, D-14476 Golm, Germany. We thank Carsten Richter (GMS Gaswechsel-Messsysteme GmbH, Berlin, Germany) for fruitful discussions and excellent technical support. This work was supported by the Max-Planck society, and the Bundesministerium für Bildung und Forschung (BMBF), Grant PTJ-BIO/0312854.

Appendix A. Supplementary data

Supplementary data associated with this article can be found, in the online version, at doi:10.1016/j.phytochem.2007.03.026.

References

Abramson, F.P., McCaman, M.W., McCaman, R.E., 1974. Femtomole level of analysis of biogenic amines and amino acids using functional group mass spectrometry. Anal. Biochem. 57 (2), 482–499.

Baxter, C.J., Redestig, H., Schauer, N., Repsilber, D., Patil, K.R., Nielsen, J., Selbig, J., Liu, J.L., Fernie, A.R., Sweetlove, L.J., 2007. The metabolic response of heterotrophic Arabidopsis cells to oxidative stress. Plant Physiol. 143 (1), 312–325.

Bergström, K., Gürtler, J., Blomstrand, R., 1970. Trimethylsilylation of amino acids. 1. Study of glycine and lysine TMS derivatives with gas-liquid chromatography–mass spectrometry. Anal. Biochem. 34 (1), 74–87.

Birkemeyer, C., Kolasa, A., Kopka, J., 2003. Comprehensive chemical derivatization for gas chromatography–mass spectrometry-based multi-targeted profiling of the major phytohormones. J. Chromatogr. A 993, 89–102.

Birkemeyer, C., Luedemann, A., Wagner, C., Erban, A., Kopka, J., 2005. Metabolome analysis: the potential of in vivo labeling with stable isotopes for metabolite profiling. Trends Biotechnol. 23, 28–33.

Blaesing, O.E., Gibon, Y., Gunther, M., Hoehne, M., Morcuende, R., Osuna, D., Thimm, O., Usadel, B., Scheible, W.R., Stitt, M., 2005. Sugars and circadian regulation make major contributions to the global regulation of diurnal gene expression in Arabidopsis. Plant Cell 17 (12), 3257–3281.

Calvin, M., 1956. The photosynthetic carbon cycle. J. Chem. Soc., 1895–1915.

Calvin, M., 1964. The path of carbon in photosynthesis. In: Nobel Lectures Chemistry 1942–1962. Elsevier Publishing Company, Amsterdam, pp. 618–644.

Dauner, M., Sauer, U., 2000. GC–MS analysis of amino acids rapidly provides rich information for isotopomer balancing. Biotechnol. Prog. 16, 642–649.

DeJongh, D.C., Radford, T., Hribar, J.D., Hanessia, S., Bieber, M., Dawson, G., Sweeley, C.C., 1969. Analysis of trimethylsilyl derivatives of carbohydrates by gas chromatography and mass spectrometry. J. Am. Chem. Soc. 91 (7), 1728–1740.

Desbrosses, G.G., Kopka, J., Udvardi, M.K., 2005. *Lotus japonicus* metabolic profiling. Development of gas chromatography–mass spectrometry resources for the study of plant–microbe interactions. Plant Physiol. 137 (4), 1302–1318.

Erban, A., Schauer, N., Fernie, A.R., Kopka, J., 2006. Non-supervised construction and application of mass spectral and retention time index libraries from time-of-flight GC–MS metabolite profiles. In: Weckwerth, W. (Ed.), Metabolomics: Methods and Protocols. Humana Press, Totowa, pp. 19–38.

Fernandez, C.A., Des Rosier, C., Previs, S.F., David, F., Brunnengraber, H., 1996. Correction of ^{13}C mass isotopomer distributions for natural stable isotope abundance. J. Mass Spectrom. 31, 255–262.

Fernie, A.R., Geigenberger, P., Stitt, M., 2005. Flux an important, but neglected, component of functional genomics. Curr. Opin. Plant Sci. 8, 174–182.

Fiehn, O., Kopka, J., Dormann, P., Altmann, T., Trethewey, R.N., Willmitzer, L., 2000a. Metabolite profiling for plant functional genomics. Nat. Biotechnol. 18, 1157–1161.

Fiehn, O., Kopka, J., Trethewey, R.N., Willmitzer, L., 2000b. Identification of uncommon plant metabolites based on calculation of elemental compositions using gas chromatography and quadrupole mass spectrometry. Anal. Chem. 72, 3573–3580.

Gibeaut, D.M., Hulett, J., Cramer, G.R., Seemann, J.R., 1997. Maximal biomass of *Arabidopsis thaliana* using a simple, low-maintenance hydroponic method and favorable environmental conditions. Plant Physiol. 115 (2), 317–319.

Gibon, Y., Blaesing, O.E., Hannemann, J., Carillo, P., Hohne, M., Hendriks, J.H.M., Palacios, N., Cross, J., Selbig, J., Stitt, M., 2004. A robot-based platform to measure multiple enzyme activities in Arabidopsis using a set of cycling assays: comparison of changes of enzyme activities and transcript levels during diurnal cycles and in prolonged darkness. Plant Cell 16 (12), 3304–3325.

Gibon, Y., Usadel, B., Blaesing, O.E., Kamlage, B., Hoehne, M., Trethewey, R., Stitt, M., 2006. Integration of metabolite with transcript and enzyme activity profiling during diurnal cycles in Arabidopsis rosettes. Genome Biol. 7 (8). Art. 76.

Kell, D.B., Brown, M., Davey, H.M., Dunn, W.B., Spasic, I., Oliver, S.G., 2005. Metabolic footprinting and systems biology: The medium is the message. Nat. Rev. Microbiol. 3, 557–565.

Klapa, M.I., Aon, J.-C., Stephanopoulos, G., 2003. Systematic quantification of complex metabolic flux networks using stable isotopes and mass spectrometry. Eur. J. Biochem. 270, 3525–3542.

Kopka, J., 2006a. Gas chromatography mass spectrometry. In: Nagata, T., Lörz, H., Widholm, J.M. (Eds.), Biotechnology in Agriculture and Forestry. In: Saito, K., Dixon, R.A., Willmitzer, L. (Eds.), Plant Metabolomics, vol. 57. Springer-Verlag, Berlin, Heidelberg, New York, pp. 3–20.

Kopka, J., 2006b. Current challenges and developments in GC–MS based metabolite profiling technology. J. Biotechnol. 124, 312–322.

Kopka, J., Schauer, N., Krueger, S., Birkemeyer, C., Usadel, B., Bergmüller, E., Dörmann, P., Gibon, Y., Stitt, M., Willmitzer, L., Fernie, A.R., Steinhauser, D., 2005. GMD@CSBDB: The Golm metabolome database. Bioinformatics 21, 1635–1638.

Laine, R.A., Sweeley, C.C., 1973. *O*-Methyl oximes of sugars – analysis of *O*-trimethylsilyl derivatives by gas-liquid chromatography and mass spectrometry. Carbohydr. Res. 27 (1), 199–213.

Leimer, K.R., Rice, R.H., Gehrke, C.W., 1977. Complete mass-spectra of per-trimethylsilylated amino-acids. J. Chromatogr. 141 (3), 355–375.

Lisec, J., Schauer, N., Kopka, J., Willmitzer, L., Fernie, A.R., 2006. Gas chromatography mass spectrometry-based metabolite profiling in plants. Nat. Protocols 1, 387–396.

MacLeod, J.K., Flanigan, I.L., Williams, J.F., Collins, J.G., 2001. Mass spectrometric studies of the path of carbon in photosynthesis: positional isotopic analysis of C-13-labelled C-4 to C-7 sugar phosphates. J. Mass Spectrom. 36 (5), 500–508.

Ratcliffe, R.G., Shachar-Hill, Y., 2006. Measuring multiple fluxes through plant metabolic networks. Plant J. 45 (4), 490–511.

Roessner, U., Wagner, C., Kopka, J., Trethewey, R.N., Willmitzer, L., 2000. Simultaneous analysis of metabolites in potato tuber by gas chromatography–mass spectrometry. Plant J. 23, 131–142.

Roessner, U., Luedemann, A., Brust, D., Fiehn, O., Linke, T., Willmitzer, L., Fernie, A.R., 2001. Metabolic profiling allows comprehensive phenotyping of genetically or environmentally modified plant systems. Plant Cell 13 (1), 11–29.

Roessner-Tunali, U., Hegemann, B., Lytovchenko, A., Carrari, F., Bruedigam, C., Granot, D., Fernie, A.R., 2003. Metabolic profiling of transgenic tomato plants overexpressing hexokinase reveals that the influence of hexose phosphorylation diminishes during fruit development. Plant Physiol. 133 (1), 84–99.

Roessner-Tunali, U., Liu, J.L., Leisse, A., Balbo, I., Perez-Melis, A., Willmitzer, L., Fernie, A.R., 2004. Kinetics of labelling of organic and amino acids in potato tubers by gas chromatography–mass spectrometry following incubation in C-13 labelled isotopes. Plant J. 39 (4), 668–679.

Sanz, M.L., Sanz, J., Martinez-Castro, I., 2002. Characterization of *O*-trimethylsilyl oximes of disaccharides by gas chromatography–mass spectrometry. Chromatographia 56, 617–622.

Schaefer, J., Stejskal, E.O., Beard, C.F., 1975. C-13 nuclear magnetic resonance analysis of metabolism in soybeans labelled by $^{13}CO_2$. Plant Physol. 55 (6), 1048–1053.

Schaefer, J., Kier, L.D., Stejskal, E.O., 1980. Characterization of photorespiration in intact leaves using C-13 dioxide labeling. Plant Physiol. 65 (2), 254–259.

Schauer, N., Steinhauser, D., Strelkov, S., Schomburg, D., Allison, G., Moritz, T., Lundgren, K., Roessner-Tunali, U., Forbes, M.G., Willmitzer, L., Fernie, A.R., Kopka, J., 2005a. GC–MS libraries for the rapid identification of metabolites in complex biological samples. FEBS Lett. 579, 1332–1337.

Schauer, N., Zamir, D., Fernie, A.R., 2005b. Metabolic profiling of leaves and fruit of wild species tomato: a survey of the *Solanum lycopersicum* complex. J. Exp. Bot. 56 (410), 297–307.

Schwender, J., Goffman, F., Ohlrogge, J.B., Shachar-Hill, Y., 2004. Rubisco without the Calvin cycle improves the carbon efficiency of developing green seeds. Nature 432 (7018), 779–782.

Sinha, A.E., Prazen, B.J., Synovec, R.E., 2004a. Trends in chemometric analysis of comprehensive two-dimensional separations. Anal. Bioanal. Chem. 378, 1948–1951.

Sinha, A.E., Hope, J.L., Prazen, B.J., Nilsson, E.J., Jack, R.M., Synovec, R.E., 2004b. Algorithm for locating analytes of interest based on mass spectral similarity in GC×GC-TOF-MS data: analysis of metabolites in human infant urine. J. Chromatogr. A 1058, 209–215.

van Winden, W.A., van Dam, J.C., Ras, C., Kleijn, R.J., Vinke, J.L., van Gulik, W.M., Heijnen, J.J., 2005. Metabolic-flux analysis of *Saccharomyces cerevisiae* CEN.PK113-7D based on mass isotopomer measurements of 13C-labeled primary metabolites. FEMS Yeast Res. 5, 559–568.

Wagner, C., Sefkow, M., Kopka, J., 2003. Construction and application of a mass spectral and retention time index database generated from plant GC/EI-TOF-MS metabolite profiles. Phytochemistry 62 (6), 887–900.

Wahl, S.A., Dauner, M., Wiechert, W., 2004. New tools for mass isotopomer data evaluation in ^{13}C flux analysis: mass isotope correction, data consistency checking and precursor relationships. Biotechnol. Bioeng. 85 (3), 259–268.

Wittmann, C., Heinzle, E., 2001. Application of MALDI-TOF MS to lysine-producing *Corynebacterium glutamicum*. A novel approach for metabolic flux analysis. Eur. J. Biochem. 268, 2441–2455.

Yang, X., Romheld, V., Marschner, H., 1994. Effect of bicarbonate on root-growth and accumulation of organic-acids in Zn-inefficient and Zn-efficient rice cultivars (*Oryza sativa* L.). Plant Soil 164, 1–7.